Lehigh University
Lehigh Preserve

Fritz Laboratory Reports

Civil and Environmental Engineering

1961

Column strength of constructional steels, presented at the Steel Design and Engineering Seminar of the U. S. Steel Corporation, Pittsburgh, (April 1961); published as a Seminar reprint, (June 1961), Reprint No. 177 (61-5)

L. S. Beedle

T. V. Galambos

L. Tall

COLUMN STRENGTH OF CONSTRUCTIONAL STEELS

by L. S. BEEDLE
T. V. GALAMBOS
L. TALL

FRITZ LABORATORY REPRINT NO. 177
"Reprinted, courtesy of U. S. Steel Corp."

Dr. Lynn S. Beedle is presently Director of the Fritz Engineering Laboratory, Lehigh University, Bethlehem, Pennsylvania. He received a B.S. degree in Civil Engineering at the University of California at Berkeley in 1941. He served in the United States Navy from 1941 to 1947 where he taught in the Postgraduate School at the United States Naval Academy and served as Officer-in-Charge of Underwater Explosion Research at the Norfolk Naval Shipyard. In July 1947 he joined Lehigh University as a Research Engineer in the Fritz Engineering Laboratory. While at Lehigh, he received an M.S. degree in 1949 and a Ph.D. degree in 1952.

Dr. Theodore V. Galambos received his Ph.D. degree at Lehigh in 1959, and is currently Research Assistant Professor in Civil Engineering at Fritz Laboratory. He is currently engaged in research in the Structural Metals Division and is Project Director of United States Steel's sponsored project on "T-1" Steel columns.

Lambert Tall is a Research Associate in the Fritz Laboratory, and has been associated with the research project on residual stress and column instability for five years. He received his Ph.D. degree in 1961.

ABSTRACT. It is shown in this paper that consistent explanation of column behavior can be made for steels of different yield-stress levels and subjected to different manufacturing and fabrication processes. This is done by taking into account the influence of fabrication procedures such as rolling, welding, and heat treatment. This summary is restricted to the behavior of centrally loaded columns, but covers ASTM A7, ASTM A242, and USS "T-1" Steel. Wide-flange shapes, welded H- and box-shapes, and round bars were studied in the research. Appropriate use of the tangent-modulus concept and a consideration of initial out-of-straightness makes it possible to arrive at a satisfactory explanation of column load carrying capacity.

INTRODUCTION. Recent technological developments are now providing the structural engineer with a selection of steels having a wide variety of strength properties. This enables the engineer to provide more useful structures with greater economy and beauty. His creativity is challenged by his ability to choose not only members of varying sizes and shapes, but also members made up of different steels.

In the case of columns, the ready availability of steels of various yield stresses fortunately coincides with the development of rational techniques for predicting the strength of columns. These procedures take into account numerous factors not recognized or carefully studied heretofore. Although developed essentially for ASTM A7 steel columns, these procedures were necessary before the behavior of higher strength steel columns could be understood.

It is the purpose of this paper to show how variables in manufacture and heat-treatment affect the strength of columns. It will be shown that a consistent explanation of column behavior can be made for steels that have different yield stresses and that are subjected to different fabrication processes.

One of the most important factors that influence the strength of columns is the loading condition. Figure 1 shows a number of possibilities: central load and load plus moments of different intensity at the ends. At one extreme is the centrally loaded column. At the other extreme is the column bent by external moments in single curvature. The latter will support less axial load than any other condition.

Although the scope of this paper is limited to centrally loaded columns, the interaction curves shown in Figure 1 indicate how significant the loading condition can be. The figure shows the axial load-carrying capacity as influenced by bending moment, the information being presented on a nondimensional basis for a typical A7 steel wide-flange column. When the moment is zero, the column will support its maximum axial thrust. On the other hand, if the moment were to reach the full plastic value M_p, then the member would theoretically support no axial load whatever. For intermediate cases, the axial load capacity is dependent upon the way the moments are introduced. The curves (which have been confirmed experimentally) show that the difference is significant and pronounced. In fact, for the double curvature case, there is a certain range of moment for which the axial load capacity is decreased only by a small amount due to the presence of such a moment.

One might say that *all* columns have either real or accidental end moments. This is true, but it is just as evident that it would unduly penalize a moment-carrying column to attempt to take into account accidental eccentricities in the limiting no-moment case. So there is real justification in learning as much as possible about centrally loaded columns. This summary of the state of knowledge concerning such members is based primarily upon References 1, 2, and 3.

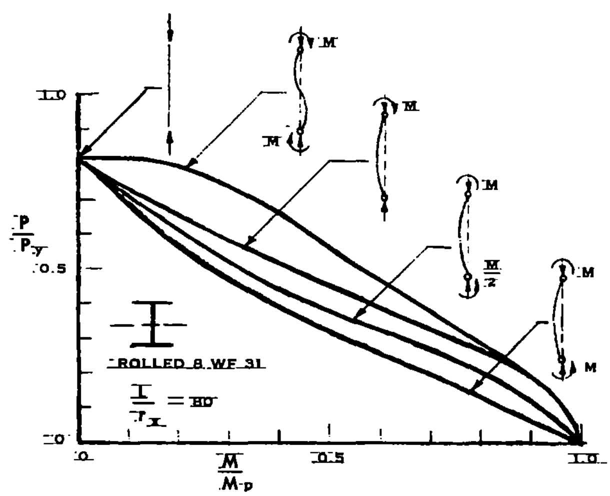

Figure 1—Influence of loading condition on an H-shaped column

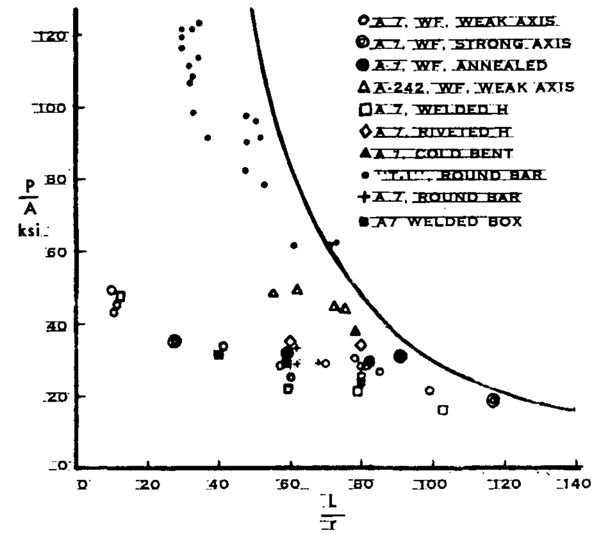

Figure 2—Results of column tests of A 7, A242, and "T-1" steel

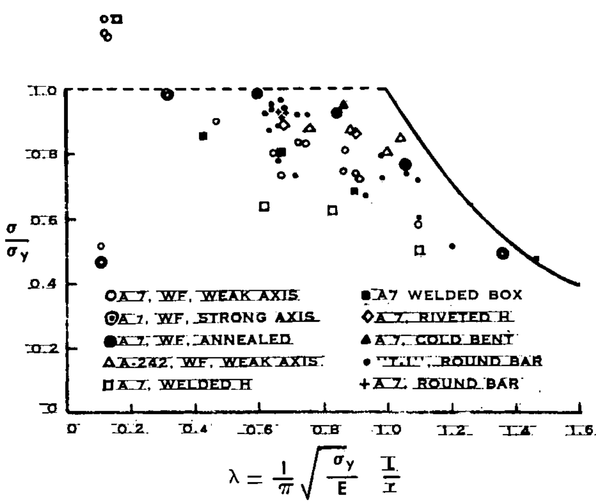

$$\lambda = \frac{1}{\pi}\sqrt{\frac{\sigma_y}{E}}\ \frac{L}{r}$$

Figure 3—Non-dimensional representation of results of column tests of A 7, A242 and "T-1" steel

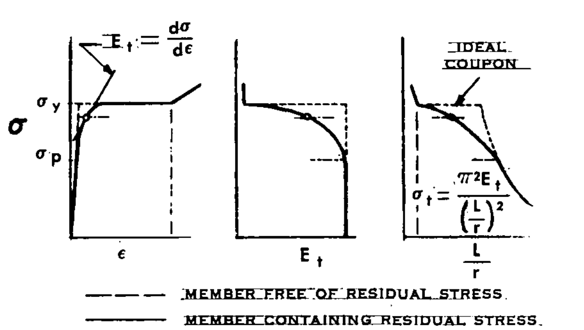

Figure 4—Influence of residual stress and strain—hardening upon the stress-strain, stress-modulus, and stress-slenderness ratio diagrams

Centrally Loaded Columns. The factors that influence the strength of centrally loaded columns are numerous and are pronounced as the scatter of points in Figure 2 suggests. The points plotted in Figure 2 represent tests of centrally loaded structural columns. The average stress is plotted as a function of $L/_r$; the curve is the Euler hyperbola for elastic column buckling and is a plot of the equation

$$P_{cr} = \frac{\pi^2 EI}{L^2} \qquad (1)$$

Even when the data is nondimensionalized to take into account the yield stress value, Figure 3, there is still more variation in column strength than would appear to be acceptable.

The importance of the variation of the material properties as a factor influencing column strength was recognized by the Column Research Council when it was formed, and it assigned to its first committee the task of determining the relationship between material properties and the strength of columns. The first pronouncement of the Council was its Technical Memorandum No. 1, "The Basic Column Formula."[4] This memorandum states that the critical or ultimate failure load of a straight, centrally loaded column is given by the tangent-modulus concept. This concept requires a knowledge of the stress-strain relationship, namely, the "material properties."

Consider first an ideal coupon free from residual stress as shown by the dotted line in Figure 4a. Since E is constant up to the yield stress level, the Euler formula would apply up to that point. Application of the tangent - modulus concept would result in a horizontal line at the yield stress level because the tangent modulus E_t is zero.

Early work has shown that rolled or fabricated shapes do not behave according to predictions based on stress-strain curves from coupons. Among other things, such shapes contain residual stresses; also, the yield level may vary across the section. As a result, the stress-strain curve ceases to be linear above a certain point.

To construct a column curve for such a material, first the tangent modulus E_t would be determined for various stress levels by using the stress-strain diagram in Figure 4a. Then a stress-vs-E_t curve would be drawn as shown in Sketch b. $E_t = E$ until the proportional limit is reached, after which it decreases to zero at σ_y. Applying the tangent-modulus concept, the resulting "column curve" of stress-vs-slenderness ratio would be obtained as shown in Sketch c.

When failure occurs in the inelastic range, the influence of a nonlinear stress-strain relationship is seen by comparing the solid line with the dashed line obtained for a member without initial stresses. In the elastic region residual stresses have no influence.

Another factor that theory has neglected until recently is strain hardening, an influence that is important for short columns. As shown in the stress-strain diagram of Figure 4a, structural carbon steel strain-hardens after the plastic strain has reached about 10 times the elastic limit value. This results in a σ versus E_t relationship that differs from the idealized case. Instead of a modulus of zero at the yield stress, $E_t \cong 750$ kilopounds per square inch (ksi), or about 1/40 the value of E. As a consequence, a column will carry a greater average critical stress than the full yield value when the slenderness ratio is less than about 15.

Thus, the strength of straight, centrally loaded columns is dependent on the stress-strain relationship of the complete cross section as a unit. The latter, in turn, is dependent on three important factors. These are

(a) The magnitude and distribution of residual stresses (which cause a lowering of the proportional limit and affect the shape of the curve above σ_p).

(b) The basic yield stress level of the material (which affects the practical upper limit of column strength).

(c) The strain-hardening modulus (which is significant for very short columns).

Columns With Initial Out-Of-Straightness. A final group of factors, interrelated with the above to a certain extent, can be classed under the heading "Initial Out-of-Straightness." Unsymmetrical residual stresses have a similar influence on the behavior of the member.

Straight, centrally loaded columns with symmetrical residual stresses will start to bend at the tangent-modulus load as shown in the upper curve of Figure 5 in which load is plotted against lateral deflection. Straight columns with unsymmetrical residual stresses (such as those produced by cold bending) will remain straight until yielding commences. The bending begins at a load that may be lower or higher than the tangent-modulus load, depending on the magnitude of residual stress. As shown by the lower curve in Figure 5, columns with initial out-of-straightness will start to deflect laterally at the start of load, with a consequent lowering of column strength.

By taking appropriate theoretical account of the influence of yield stress, residual stress (both symmetrical and unsymmetrical), strain-hardening, heat-treatment process, cross-section shape, and initial out-of-straightness, it should be possible to predict each of the test points shown in Figure 2 with sufficient accuracy.

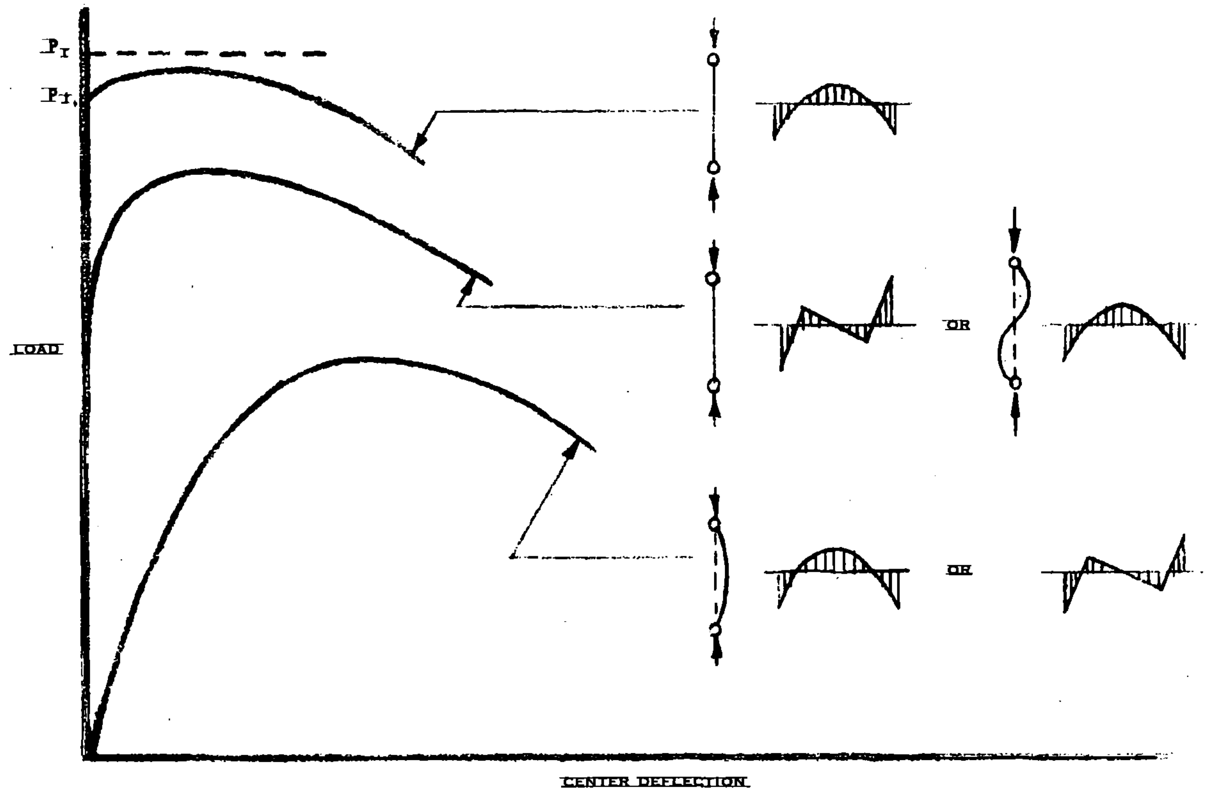

Figure 5—Behavior of columns with cooling residual stresses, "cold-bending" stresses, and initial out-of-straightness

Influence of Residual Stresses Due to Cooling After Rolling Structural Carbon Steel. Residual stresses are formed in a structural member as a result of plastic deformations. In rolled structural shapes, these deformations always occur during the process of cooling from the rolling temperature to ambient air temperature; the plastic deformations result from the fact that some parts of the shape cool much more rapidly than others and cause inelastic deformations in the slower cooling portions. The situation is similar for welded members and for heat-treated bars that are other than furnace-cooled. Members that are cold-straightened contain residual stresses as a result of the plastic bending deformations that are applied. In general, it might be stated that there are no residual stresses if there is no plastic deformation during the life of the material. Further, for elements under temperature gradient, the part to cool last will usually be in a state of tensile residual stress.

In a rolled wide flange (WF) shape, for example, as cooling continues from the rolling temperature, the tips of the flanges cool faster than the web and balance of the flanges. They become hard and resist the contraction of the hotter material where the flange joins the web and causes plastic deformations there. As a result, it would be expected that at ambient temperature the flange edges would be in a state of residual compression and the flange center in residual tension.

Of the many sets of residual measurements that have been made, Figure 6 shows the results for three WF structural carbon shapes of widely differing size and geometry. Although the variation is considerable, the general pattern in the flange is as expected. Insofar as columns are concerned, it will be seen later that the most important of the stresses are those at the flange tips. For A7 steel, the average stress measured there is about 13,000 psi in compression.

To examine the influence of these stresses, con-

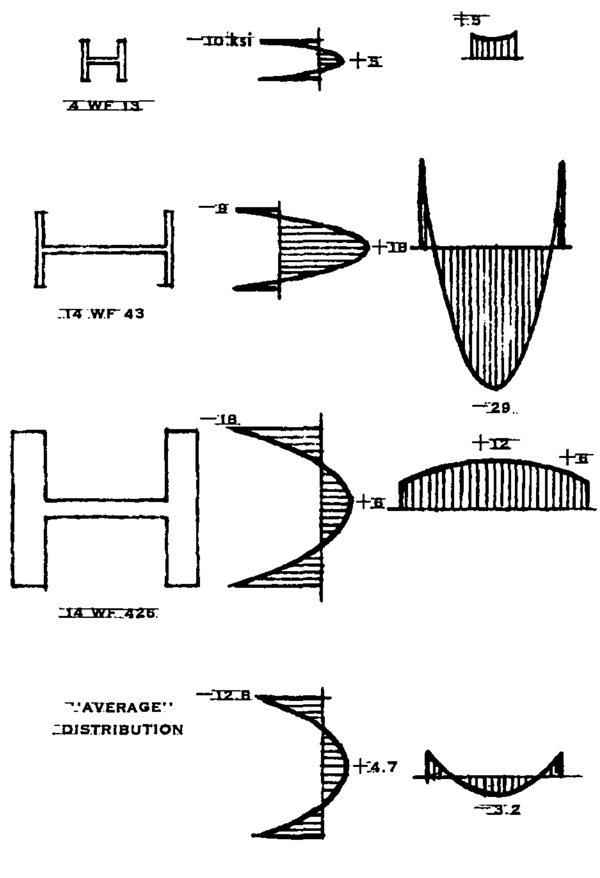

Figure 6—Residual stress distribution in WF shapes (A-7 steel)

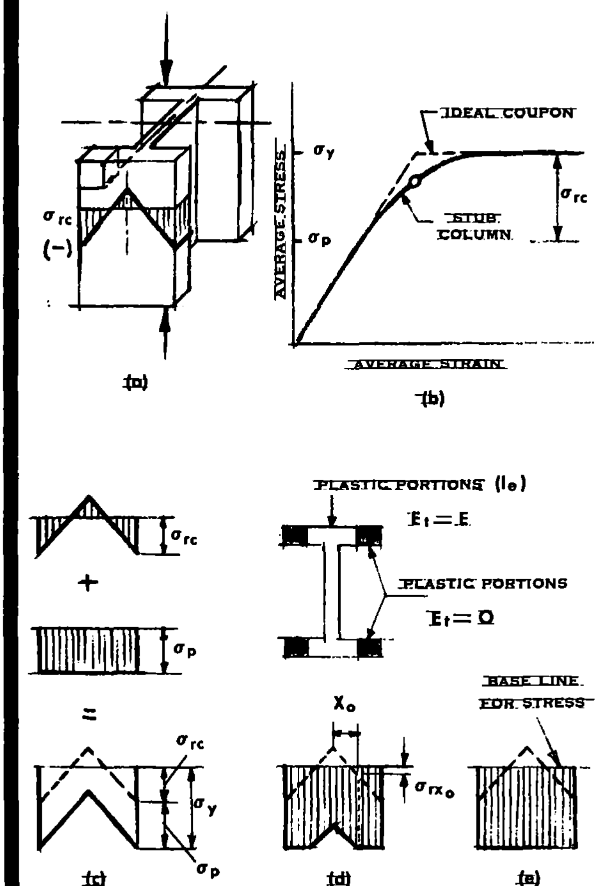

Figure 7—Influence of residual stress on stress-strain curve

sider Figure 7. The cutting of a coupon from the flange of a member relieves the residual stresses present in the member prior to sectioning. Thus the stress-strain diagram would be as shown by the dashed line in Sketch b.

If, now, the load is considered as being applied to the entire cross section containing its residual stresses, it is evident that the behavior will be linear until the applied stress becomes equal to the difference between σ_y and σ_{rc}. Then yielding will commence at the flange tips. A linear distribution of residual stress has been indicated. As shown in Sketch b, the stress-strain curve will remain linear as long as the applied stress is less than σ_p.

When more load is applied, the average stress and average strain are no longer proportional to one another because of yielding of the flange tips. Thus a nonlinear stress-strain relationship results for the section as a whole. The circle in Sketch b corresponds to distribution, d, the flange edges having yielded.

After yielding has penetrated across the entire section, the stress distribution is identical to that of a shape containing no residual stresses. In effect, they are "wiped out" and have no influence on the yield stress level.

The curved portion of the stress-strain diagram in Sketch b, then, reflects the influence of residual stress. It causes a marked reduction in the proportional limit (to about 20 ksi for A7 steel) and a consequent reduction in the tangent-modulus values when this stress is exceeded.

The way to confirm this experimentally is to test an entire cross section, or "stub column." Such a test is shown in Figure 8. The member is short enough to prevent column instability but long enough to retain the residual stresses. The 14WF426 shape is being compressed in a 5-million-pound capacity hydraulic testing machine. The load at a yield stress level of 33 ksi would be about 4 million pounds. Such a test not only reflects the influence of residual stress, but also automatically averages out the difference in yield stress for different parts of the cross section.

A typical stress-strain curve for such a stub-column test is shown in Figure 9. The behavior of an isolated coupon is shown by the dashed line. The experimental points connected by the curve are from the test of the whole section or "stub column." Very good correlation is obtained with the earlier predictions (Figure 7) for this 18WF105 member.

It is possible to examine the strength of columns containing "cooling" residual stresses through use of the tangent-modulus concept. The tangent-modulus formula is:

$$P_t = \frac{\pi^2 E_t I}{L^2} \qquad (2)$$

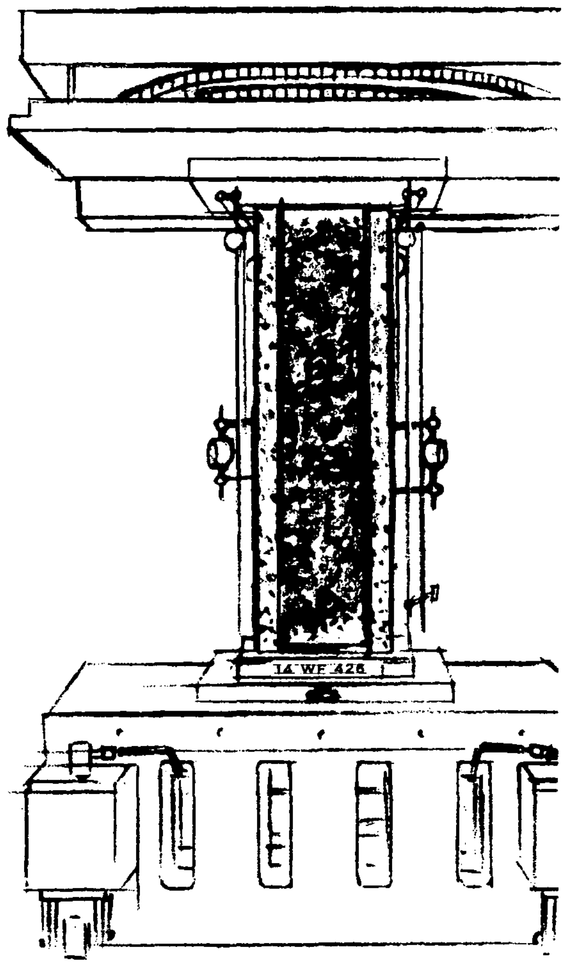

Figure 8—Testing a "stub column" on 5-million-pound machine at Fritz Engineering Laboratory, Lehigh University.

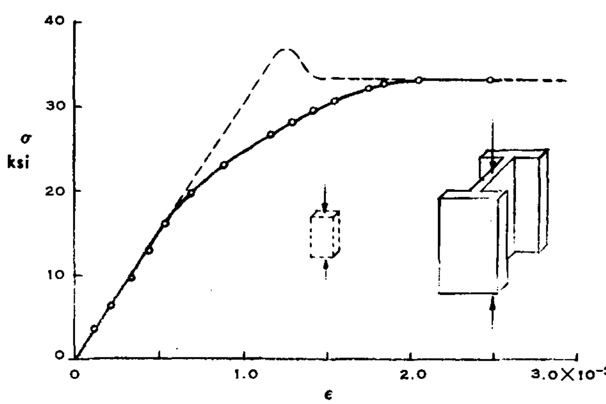

Figure 9—"Stub column" stress-strain curve for as-delivered material in comparison with coupon test result

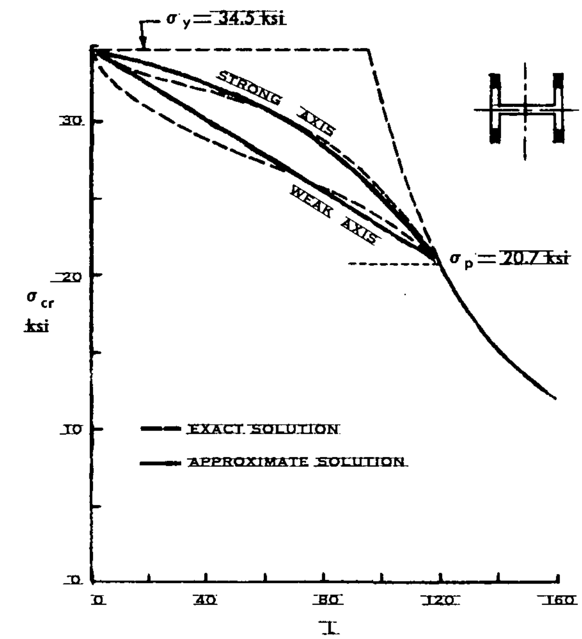

Figure 10—Column curves for WF shape with cooling residual stress

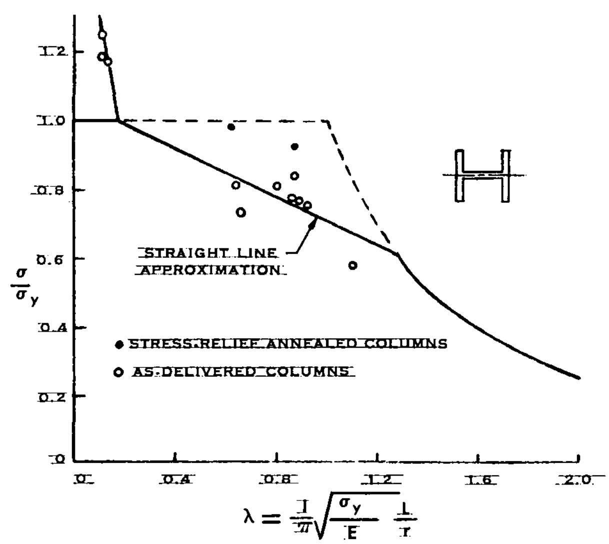

Figure 11—Results of column tests of A 7 steel and straight-line column formula (weak axis)

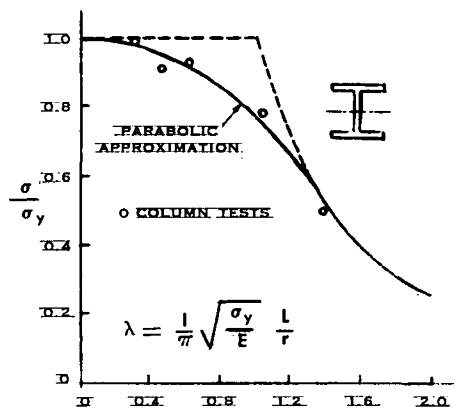

Figure 12—Results of column tests of A 7 steel and parabolic column curve (strong axis)

in which E_t is determined directly from the stress-strain curve. Equation 2 is "exact" only for the special case of a rectangle bent about the weak axis. Without going into detail, the real key to the solution lies in a consideration of the moment of inertia of the yielded cross section. It has been shown that this moment of inertia may be expressed *in terms of* E_t.

Consider the partially yielded cross section shown in Figure 10. $E_t = E$ for the elastic portion, but $E_t = 0$ for the yielded tips. In effect, it is a new cross section of which the reduced moment of inertia, I_e, is that of the portion which remains elastic. Thus, the buckling equation is:

$$P_t = \frac{\pi^2 E I_e}{L^2} \quad (3)$$

and, as noted above, I_e may be expressed as a function of E_t.

There is a difference in strength depending on the flexure axis. When flexure occurs about the weak (y-y) axis, the material most remote from the neutral axis does not contribute to the moment of inertia since it has yielded. The reduction is not so drastic for a column bent about the strong axis, and this tendency is shown in Figure 10. The lower curves are for flexure about the weak axis of an H-section, and the upper curves are for flexure about the strong axis.

The dashed lines in each case represent so-called "exact" solutions, solutions derived from the actual residual stress distributions. It will be noted that the curve for buckling about the strong axis is approximately parabolic in shape; for buckling in the weak direction, the curve may be approximated by a straight line.

Figure 11 shows that the results of weak-axis column tests are in good agreement with the straight-line approximation previously mentioned. The circles show the maximum load the columns carried. The coordinates are nondimensionalized in order that variation in E and σ_y could be eliminated. Also shown are the results of tests of stress-relief annealed columns (solid dots). Clearly their strength is well above that of the as-delivered members. Two tests at small L/r values confirm the influence of strain hardening. Figure 12 similarly shows the results of column tests in which flexure was about the strong axis in comparison with the parabolic approximation of Figure 10. Again there is good correlation between theory and tests.

Higher Strength Steels. The next question is, how do the material properties of higher strength steels compare with A7, and do they influence column performance in a similar way?

Figure 13a shows comparative curves of constructional alloy (USS "T-1"), high-strength low alloy (ASTM A242), and structural carbon

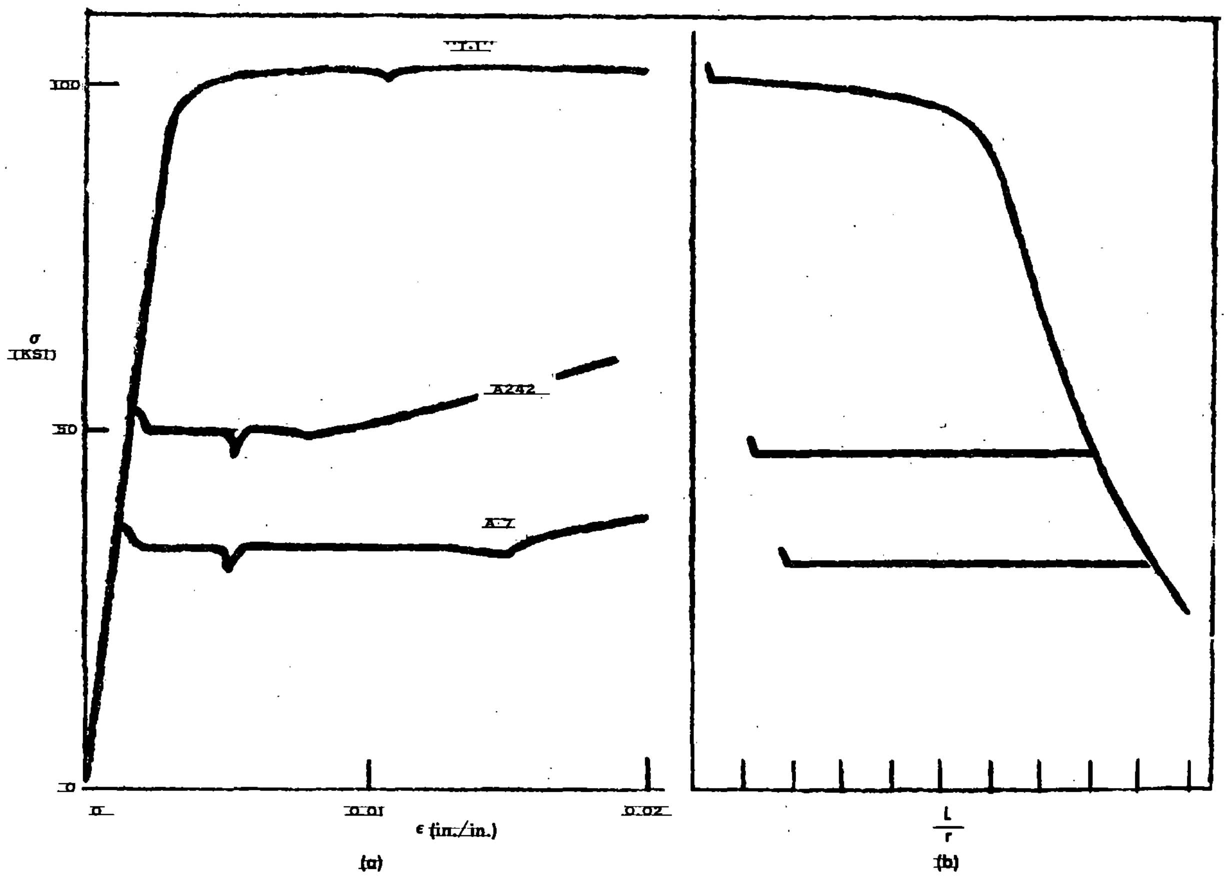

Figure 13—Comparative stress-strain curves (a) and column curves (b) for "T-1", A242, and A 7 steels

(ASTM A7) steels. They represent the autographic record of typical tension coupon tests conducted at Fritz Laboratory. The similarities in the three steels are as follows:

(a) The abrupt change at yield.
(b) The relatively long plateau of strain during which the stress remains constant with increasing strain.
(c) Sensitivity to dynamic effects. The dips represent points where the testing machine was stopped; if the machine had been operated at a faster strain rate, the corresponding stress would have been higher.

Other than strength, differences in the three steels are as follows:

(a) The absence of an upper yield point in "T-1" Steel. (In the final analysis, this is of no consequence because the residual stress effect "wipes out" any upper yield point that exists in the other steels.)
(b) The yield plateau in A242 and in A7 steel is usually horizontal up to strain hardening. The "T-1" plateau has a slight slope.
(c) Both A7 and A242 steel strain-harden after considerable strain and have (from limited tests on A242 steel) similar values of the strain-hardening modulus. ($E_t \cong$ 750 ksi). "T-1" Steel on the other hand has a continuously rising curve with $E_t \cong 100$ ksi.

Omitting for the moment the influence of residual stresses, the column curves for the three steels are shown in Figure 13b. It reflects the similarities and the differences. The column curves are constructed on the basis of the static yield stress mentioned above: the sudden transition from elastic to plastic region, the strain-hardening of A7 and A242 steel, and the gradual rise of "T-1" Steel column strength as $L/_r$ approaches zero.

Of next interest are the magnitude and distribution of residual stresses due to air-cooling of higher strength steels. Measurements have been made not only on A7 but also on A242 steels. They will shortly be made on "T-1" Steel, but in advance of the measurements, calculations have been made on what the expected distribution and magnitude might be. The results are shown in Figure 14 for 3 wide-flange shapes of different geometry and size (8WF31, 12WF50, and 12WF65). It shows that the residual stress magnitude and distribution is about the same in the two measured steels. The theoretical examination for "T-1" Steel also suggests that the magnitude and distribution of residual stress is not influenced by the yield stress level. Of much greater importance is the geometry of the cross section.

The yield stress level σ_y is also shown in Figure 14. As shown, $\sigma_p = \sigma_y - \sigma_{rc}$. Since σ_{rc} does not vary, a comparison of the three steels indicates that the proportional limit ($\sigma_p = \sigma_y - \sigma_{rc}$) increases as σ_y increases. Thus, the influence of residual stress should not be as pronounced in the higher strength steels.

The corresponding average stress-strain relationship is shown in Figure 15a on a nondimensional basis. The proportional limit would be the lowest for the A7 steel. The "T-1" Steel should have the highest proportional limit. The column curve in Figure 15b shows diagrammatically that the higher the yield stress level, the stronger will be the column (relatively speaking). Thus, we can expect that in the higher strength steels the influence of residual stress will be less pronounced.

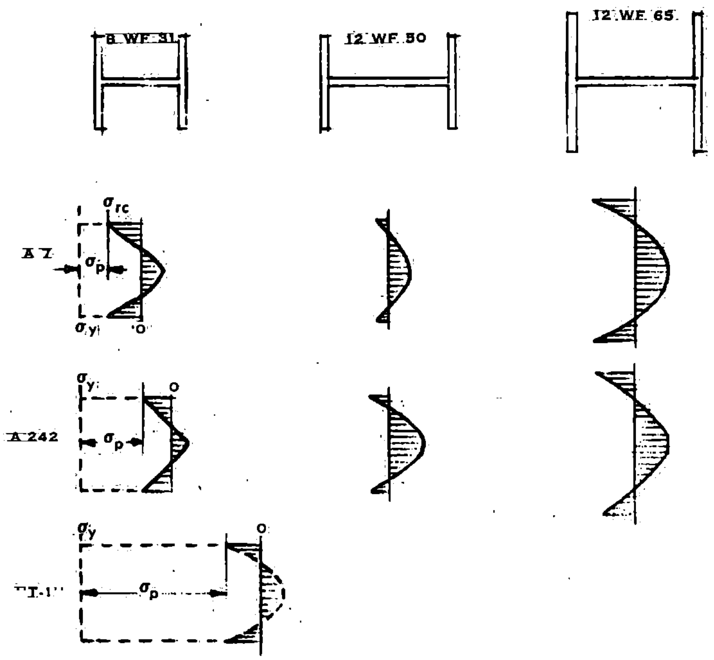

Figure 14—Residual stresses in rolled shapes of differing geometry and yield strength

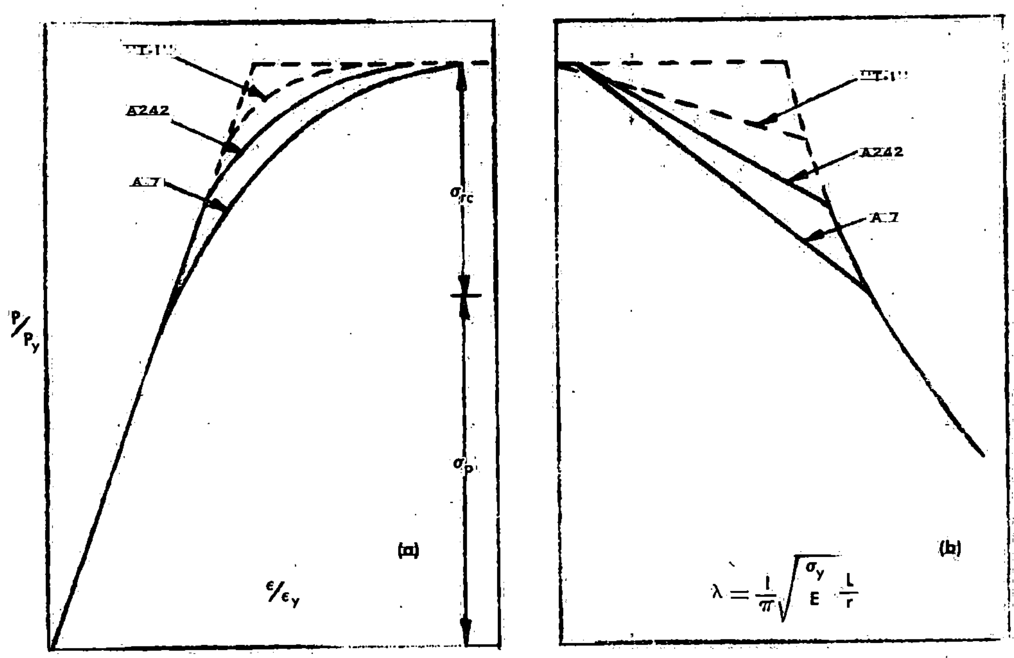

Figure 15—Column curves of different steels as affected by residual stress

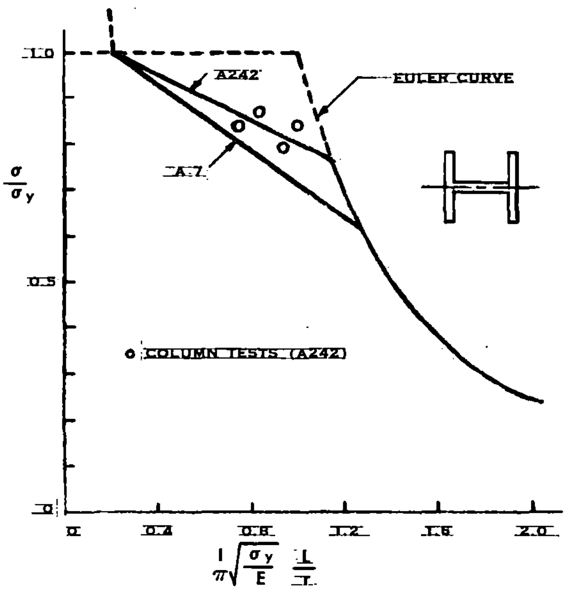

Figure 16—Column curves and test results for A242 steel compared with A 7 steel

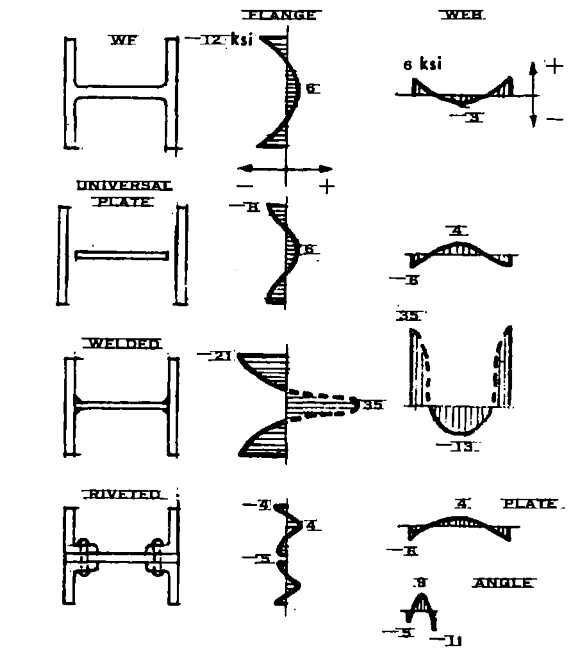

Figure 17—Residual stress patterns compared in rolled members, in plates, and in welded and riveted members

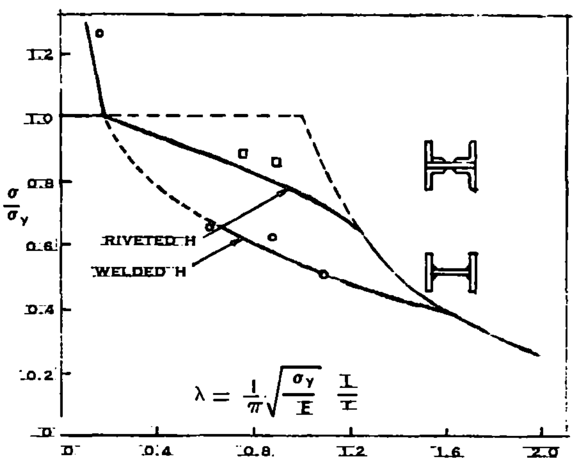

Figure 18—Test results and column curves for welded and riveted members (weak axis)

Figure 16 shows that these predictions are confirmed by actual weak-axis column tests on A242 steel, with the same shapes for which residual stresses shown in Figure 14 were measured. The average curve for A7 steel affords a basis for comparison. The per cent reduction in column strength due to this factor is less for the stronger material.

Influence of Welding Residual Stresses. Some of the data in Figure 2 were the results of tests on welded shapes. Two questions arise with regard to such members: How do welding residual stresses compare with those set up because of cooling after rolling? And how are these stresses influenced by the geometry of the shape?

Figure 17 shows a comparison of residual stresses in WF shapes, in universal mill plates, and in welded and riveted sections. The as-rolled plates contain significant residual stresses due to cooling after rolling. The welding process introduces high tensile residual stresses at the flange-web juncture (they frequently approach the yield stress of the weld metal), and this gives rise to compressive stresses that are higher than those encountered for the rolled shapes—at least for these tests. In these tests, plates 9 inches by ¾ inch and 9 inches by ½ inch in size were joined with 5⁄16-inch fillet welds. The riveted shape has only those stresses that were present in the angles and plates prior to fabrication, and these stresses are rather low.

Tests confirm the results that would be predicted on the basis of measured residual stresses. Figure 18 indicates that the riveted columns with low residual stresses exhibited relatively higher column strength. The welded columns with higher compressive residual stresses at flange tips gave lower strength. In fact, there is a greater reduction than has been observed in the case of rolled shapes.

The magnitude and distribution of welding residual stresses are markedly influenced by the geometry. Further work was, therefore, required on members with cross-sectional shapes other than the H-section. It was expected, for example, that the use of welded H-shape columns would be replaced more frequently by "box" sections and that these would undoubtedly show a higher strength.

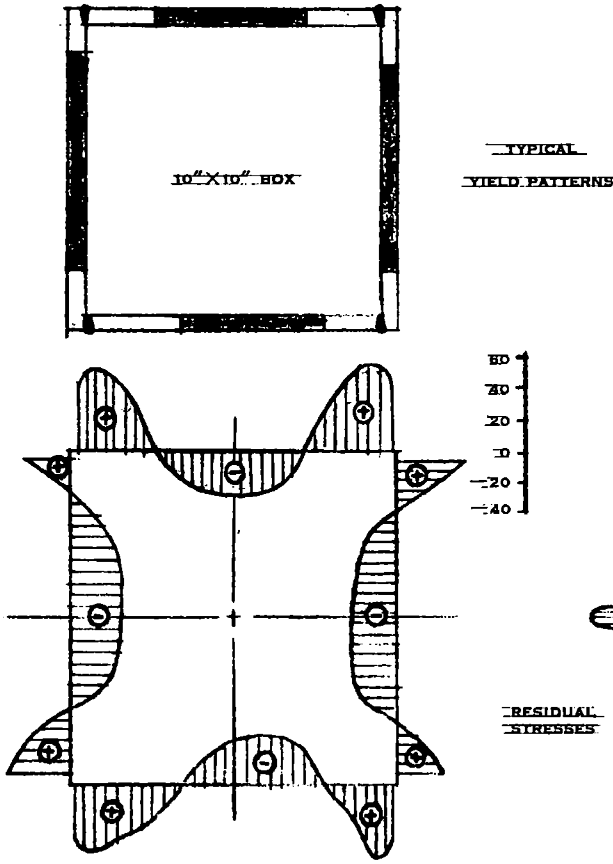

Figure 19—Residual stresses in welded box shape compared with those in welded H-shape

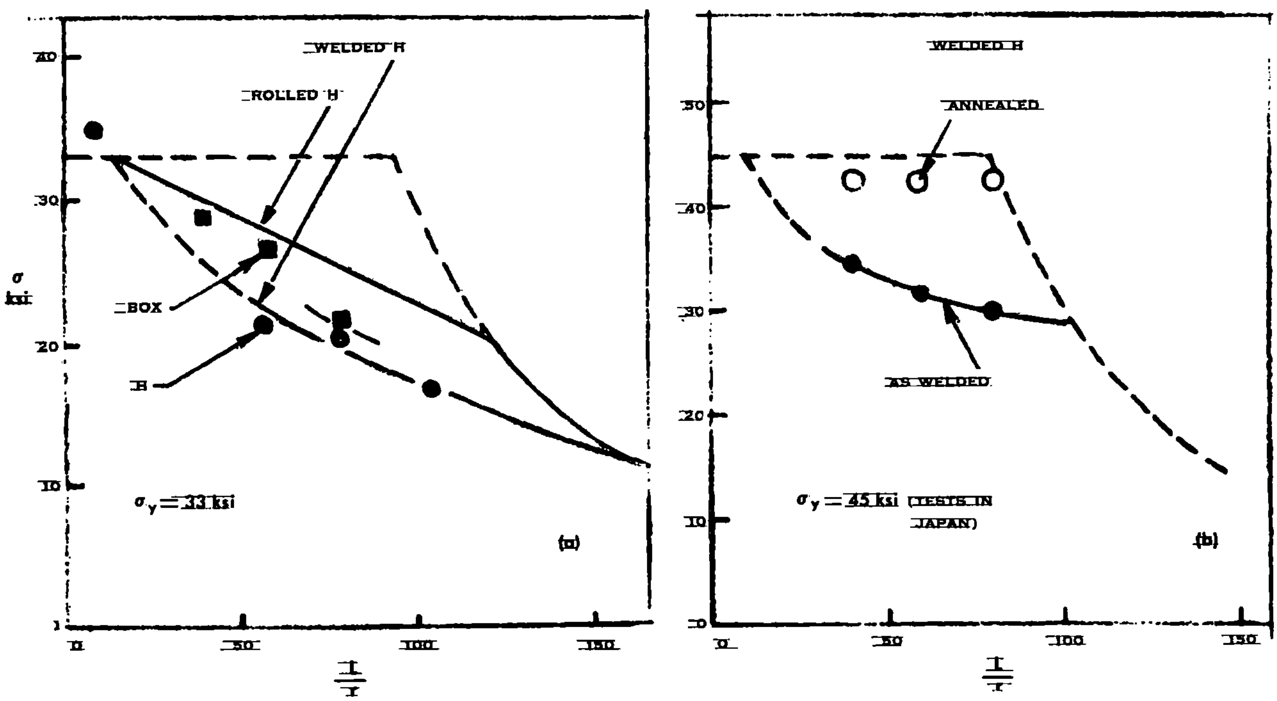

Figure 20—Results of tests on welded box and H-columns

This work is currently underway, but enough has been learned to show that the estimate was correct—in part, at least. Figure 19 shows the residual stresses caused by welding of a box shape. The stresses at the weld are above the yield point of the base metal (because of the greater strength of the weld metal). To balance this, the compressive stresses are also fairly high (about 30 ksi). For comparison, the residual stresses in a welded H-shape are also shown. The important point to note is that first yielding under compression load does not take place at the corners (corresponding to the tips in an H-shape). Thus, in spite of the high compressive residual stresses, the elastic moment of inertia is more favorable for column performance than in the case of a welded H-shape bent about the weak axis.

In Figure 20a are shown the results of a few tests of welded box columns. The curve for rolled H-shapes is the upper one (average weak axis tests). The theoretical ultimate strength and observed test results for the welded H-shapes are the lowest groups. The other points are for the box shapes. As expected, they are stronger, in fact, approaching the strength of the rolled members. The longest test column has the greatest initial curvature. The short line near the test point is the predicted value when this measured out-of-straightness is considered.

At a later date, box columns of higher strength steel will be tested in the Lehigh program. In the meanwhile, the only known tests on high-strength welded columns are from Japan. These are welded H-shapes with results shown in Figure 20b. As before, tests of stress-relief annealed members practically reached the yield value. Also, as in the case of rolled members, the welding residual stress effect appears to be less pronounced for the higher strength steel.

ROUND COLUMNS

"Cooling" Residual Stresses. The following group of columns to be discussed are round columns of "T-1" Steel, a quenched and tempered constructional alloy steel. These are members that are frequently used for the main legs of television towers. An example is shown in Figure 21. Round columns were studied in a program which is being sponsored by U. S. Steel Corporation to determine the effect of heat-treatment and cold bending on the residual stress and thus on the column strength. This study will also illustrate the effects of initial out-of-straightness.

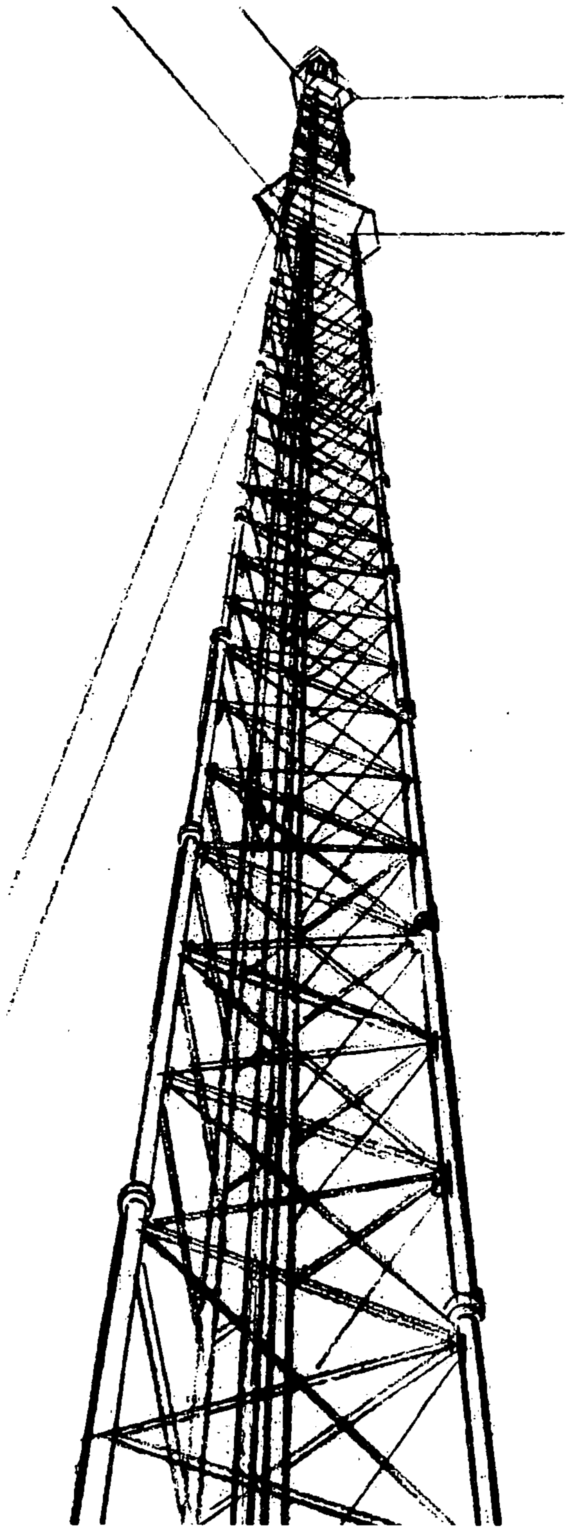

Figure 21—Round columns of USS "T-1", a quenched and tempered constructional alloy steel, are frequently used for the main members of television towers.

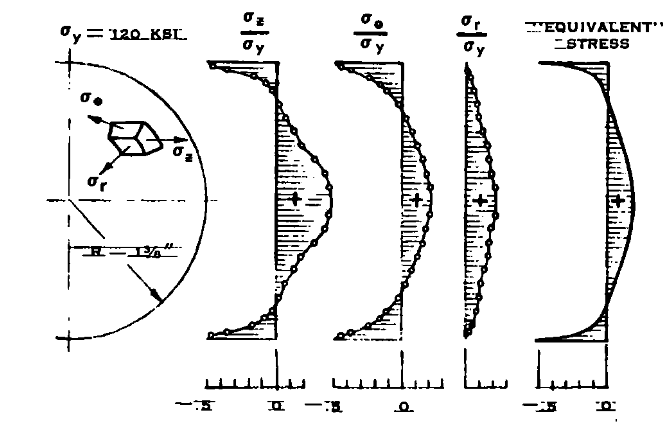

Figure 22—Residual stresses in round "T-1" steel bars (quenched, tempered and quenched from tempering temperature)

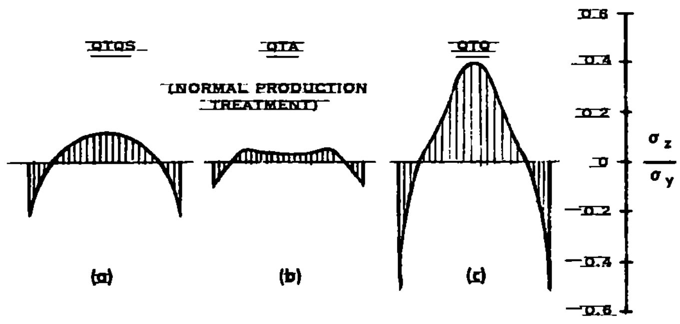

Figure 23—Influence of final heat-treatment process on residual stresses

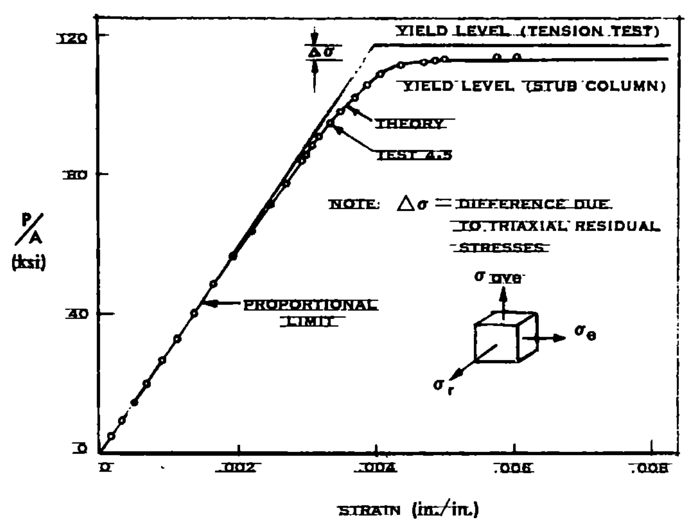

Figure 24—Stub-column test of round bar containing residual stress

The first illustration in this group, Figure 22, shows the types of residual stresses present in round bars due to heat-treatment. The stresses shown have been measured in a 2¾-inch-diameter bar, which had been cooled from the tempering temperature by water quenching. Because of this, the residual stresses are rather high (more than half the yield stress in this case).

Because the bar is solid, the residual stress distribution can no longer be assumed to be uniaxial, as for thin-walled members (such as the WF sections), but it is triaxial. There are longitudinal, tangential, and radial stresses (σ_z, σ_θ, and σ_r in the figure). The radial stresses are small. They are the stresses that are necessary to hold the tangential stresses in equilibrium. The "equivalent stress" shown in Figure 22 was used in the analysis rather than the separate effects of the three different residual stresses.

Another variable in these steels is the method of heat-treatment. Figure 23 shows what might be expected for different final treatment conditions. It compares bars that have been (a) quenched, tempered, and stress-relieved; (b) quenched, tempered, and air-cooled from the tempering temperature; or (c) quenched, tempered, and quenched from the tempering temperature. Of these, the quench, temper, and air-cool treatment is the normal production treatment. Figure 23 shows that the maximum compressive stress at the edges is from 10 to 20 ksi when the final treatment is stress-relieving or air-cooling. When the final treatment is quenching, the stresses are very high (up to 80 ksi for these tests).

The residual stresses seen in previous figures influence the behavior of a stub column in much the same way as observed for stub columns of wide-flange shapes. Figure 24 shows the results of such a test. The specimen was a 2¾-inch round bar. (Similar information has been obtained for 7½-inch round bars.) The final treatment operation was quenching from the tempering temperature and should reflect the largest influence that might be observed. The calculated curve was based on residual stress measurements and the measurement of the static yield stress*. The points represent observations from the stub-column test, and the agreement is excellent. Because of the relatively small area along the outer surface that is under high stress, the deviation in the stress-strain relationship is less pronounced than was observed in the case of structural carbon steel.

Of note is the fact that the stub-column curve does not quite reach the yield stress of a tension

*The yield stress at a zero strain rate.

coupon in the range of strain shown in Figure 24. The reason for this is the triaxial stress effect. It is clear that the influence is not great, and eventually when the stub column is sufficiently strained, the strength reaches the coupon value.

Figure 25 shows the column curves which result from application of tangent-modulus theory to the "T-1" stub-column curves for different heat-treatment. (It has been shown that the failure load is proportional to $\left(\frac{E_t}{E}\right)^2$ for round bars.) In the upper curve, the final treatment after tempering is a stress-relieving. In the next curve, the final treatment is air-cooling. In the lower curve, the final treatment is quenching. The test results show the correlation obtained.

The agreement is not too good in some cases, and the reason for this is initial out-of-straightness (which will be discussed later) and lack of symmetry of residual stresses.

Initial Out-Of-Straightness. The final group of centrally loaded columns for which test results are shown in Figure 2 were those with some of the effects discussed earlier. This includes the columns that initially were not perfectly straight and those which contain unsymmetrical residual stress patterns. Both of these effects introduce eccentricity into the problem. The effect was shown diagrammatically in Figure 5.

In Figure 26, actual test data are correlated with theoretical predictions. Referring to Sketch a, a straight column with residual stresses will start to deflect at the tangent-modulus load. There will be a small increase (depending on residual stresses and shape of cross section), and then the load drops. A column with initial out-of-straightness, Sketch a, will start to deflect from the very beginning. The result is a lower strength.

Similar behavior is observed for the test of a 7½-inch bar containing both initial out-of-straightness and an unsymmetric residual stress, Sketch b.

Sketch c shows a similar effect for a welded box shape. In this case, the residual stresses were almost symmetrical. The column was centered under load, and thus, the effect of measured initial out-of-straightness did not become evident until substantial load had been applied to the member.

The effect of out-of-straightness in members with low residual stresses (stress-relieved bars) is shown in Figure 27a. The theoretical ultimate strength curves for $\frac{\delta_o}{r}$ = 0, 0.02, and 0.05 assume no residual stress. Evidently, the presence of a small amount of out-of-straightness results in a substantial reduction in column strength. Test results for a number of "T-1" Steel and structural

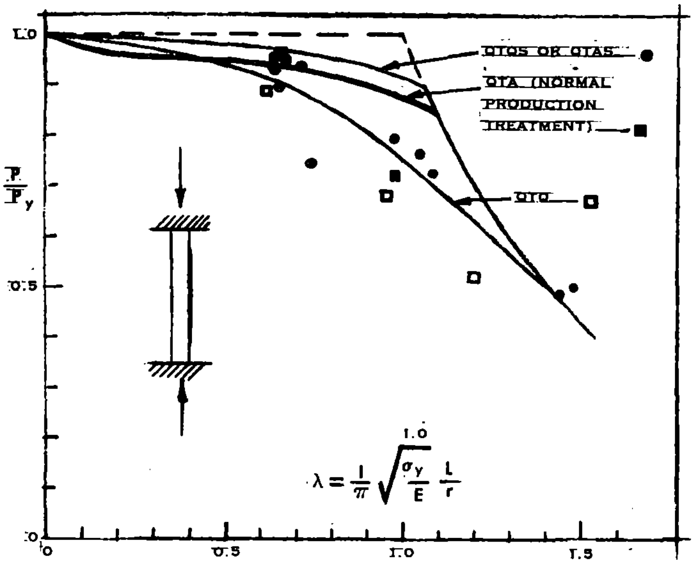

Figure 25—Column curves and test results for "T-1" steel with different treatments

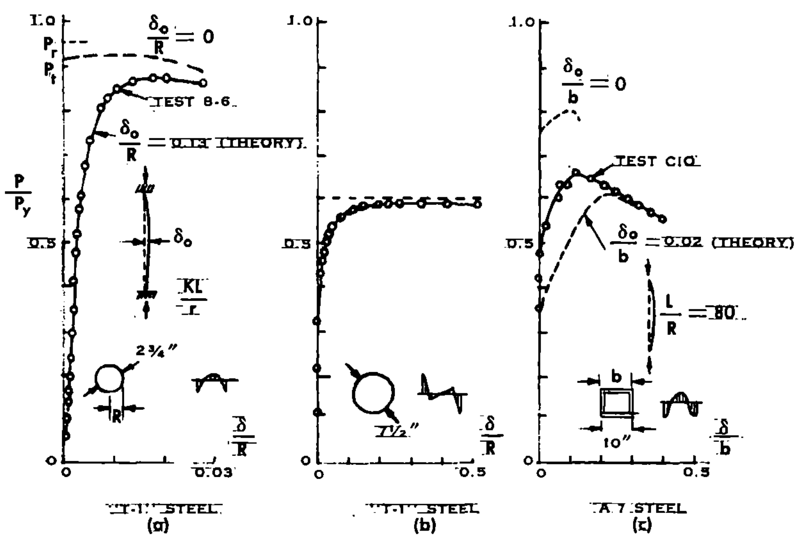

Figure 26—Effect of initial imperfections on column strength

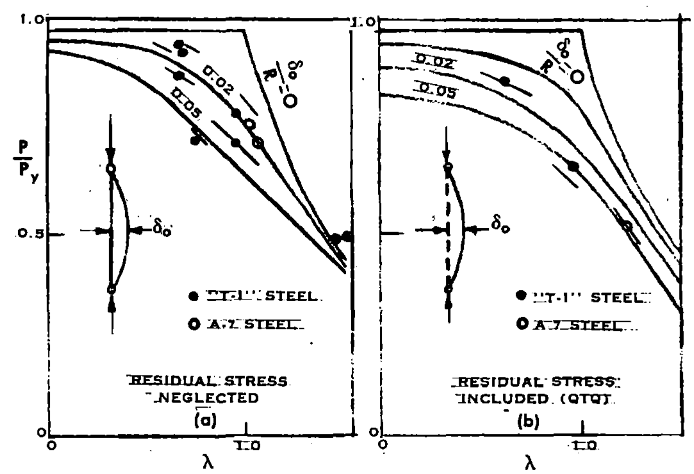

Figure 27—Effect of out-of-straightness on column strength

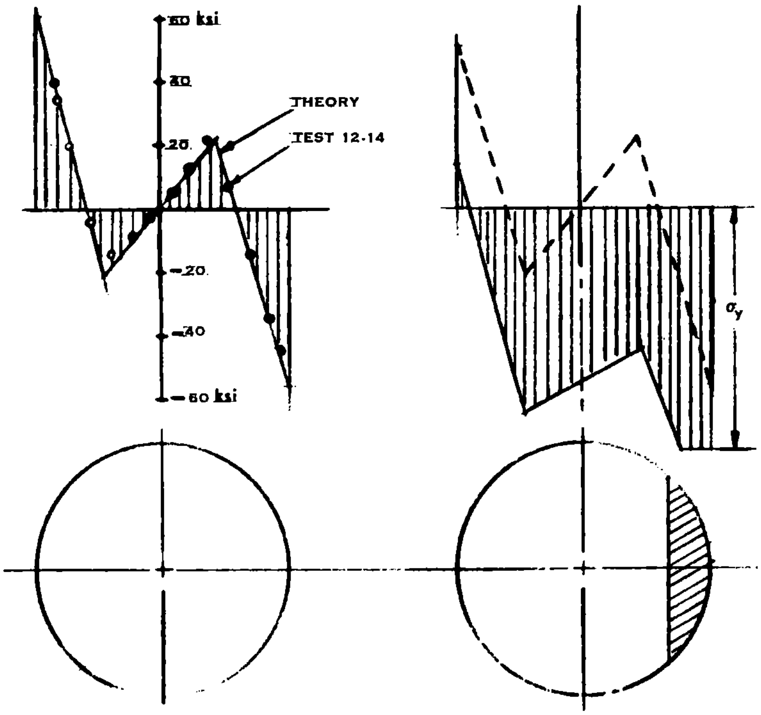

Figure 28—Residual stresses in cold-bent bars

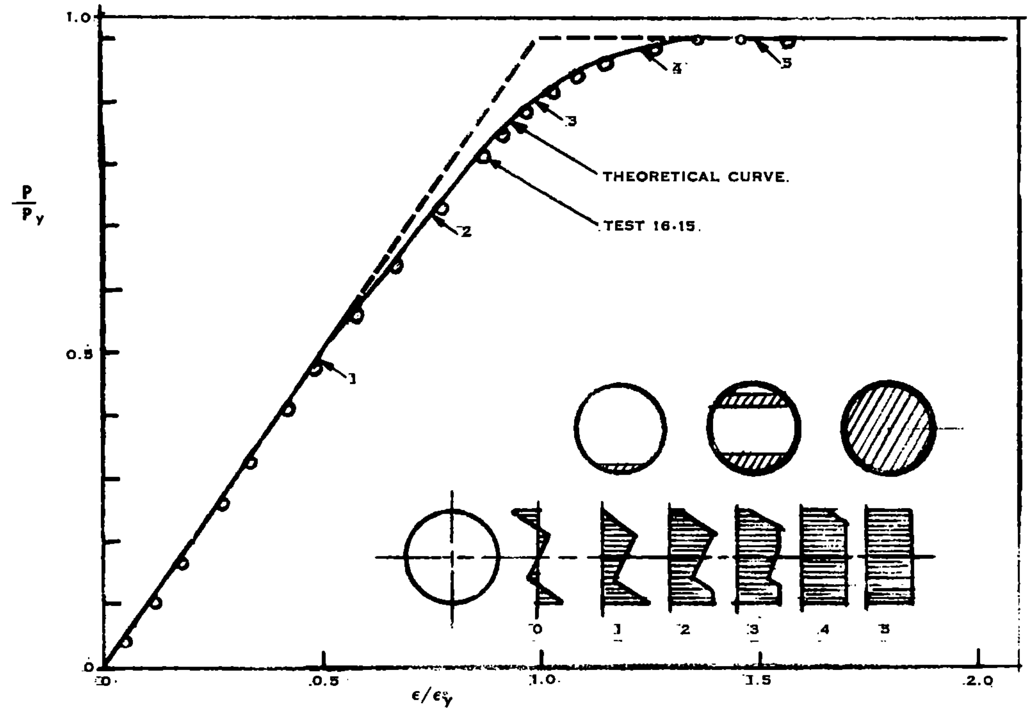

Figure 29—Stub-column test of round bar after cold-bending

carbon steel columns are shown along with a short segment of the theoretical curve for the apparent out-of-straightness. The agreement is very good.

Since the effect of out-of-straightness is pronounced (as is also the residual stress effect), in order to get a close prediction of the strength of most test columns, it will be necessary to consider the influence of both of these factors.

Figure 27b shows first the influence of symmetrical residual stresses for "T-1" Steel bars quenched from the tempering temperature. It is the lowest tangent-modulus curve given in Figure 25. For initial deflections of $\frac{\delta_o}{r}$ = .02 and .05, the strength is lowered as shown in the corresponding curves. The test points, shown in the same way as before, indicate the good agreement that was obtained with predictions. As expected, in these "T-1" Steel columns in which the residual stress effect is less pronounced than for A7 steel columns, the effect of initial out-of-straightness becomes more significant in the "knee" of the column curve.

The remaining effect to be considered is that of cold-bending. In the left portion of Figure 28 are seen the stresses that are set up as a result of straightening. On one side of the member the stresses are compressive and on the other side they are tensile. These stresses may be predicted by a plastic analysis, and the comparison of the measured residual stresses with the predicted distribution shows that the agreement is very good.

In the right portion of Figure 28 is seen the effect of adding an axial thrust sufficient to cause yielding. The addition of a compressive stress causes yielding to occur on the "compressive" side. The shaded portion shows the corresponding yielded zone in the round bar. As a result of this yielding on one side, bending commences and we have an eccentric column.

Figure 29 is a load-versus-strain curve obtained from the stub-column test of a member which had been cold-straightened. The initial residual stress distribution is shown followed by various stress patterns that correspond to the attainment of certain limiting stress conditions in the cross section. The corresponding points in the load-strain curve are indicated. Gradually, the section yields until finally the full cross section is yielded. Here, again, there is unusually good agreement between the theoretical prediction and the test measurements as shown by the points.

Column tests have also been conducted on cold-straightened members, and the results confirm the theoretical predictions.

SUMMARY. In summarizing, research on centrally-loaded constructional steel columns has shown that

1. Residual stresses due to cooling after rolling, due to welding, due to cold bending, and due to various heat-treatment processes have a pronounced influence on the stress-strain curve, Figure 9, and generally decrease the load-carrying capacity of columns, Figures 11, 20, and 25.

2. Residual stresses in rolled shapes do not appear to be influenced by the level of yield stress, Figure 14. Thus, the higher strength steel columns show less reduction in strength because of residual stress, Figures 15 and 16.

3. Residual stresses due to full strength welds are usually greater than those set up due to cooling after rolling, Figure 19. As a result, the strength of welded H-shapes is less than that of rolled WF shapes, Figure 20a. However, since geometry plays a significant role, tests show that box shapes give higher strength. Further research on the influence of geometry and of weld size will shed further light on the problem.

4. The same analytical techniques used for A7 and A242 steels may be applied to solid round columns of "T-1" Steel for the predicting of "stub-column" strength, Figures 24 and 29, and the tangent-modulus load, Figure 25.

5. Surface residual stresses due to quenching of round bars from the tempering temperature are high and may be predicted rather well, Figure 22. When the final treatment is air cooling from the tempering temperature or stress relieving, the stresses are markedly reduced, Figure 23, as is their influence, Figure 25.

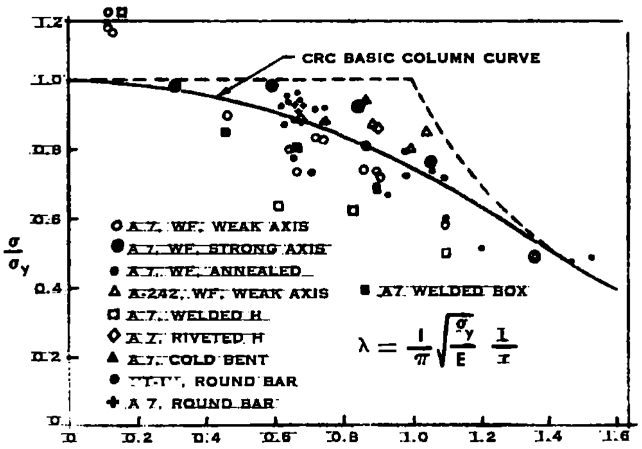

Figure 30—Column tests of different steels in comparison with "basic column curve"

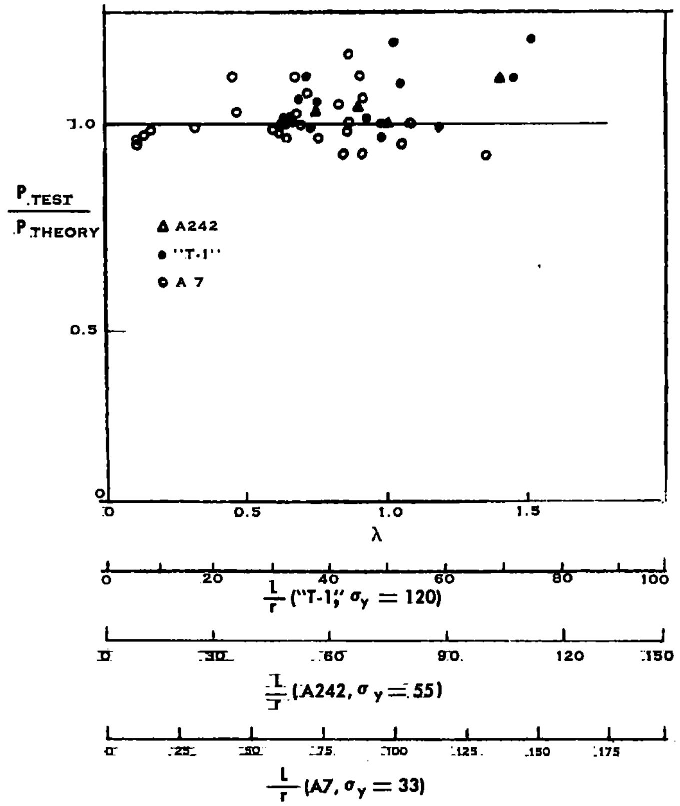

Figure 31—Correlation of available theory and tests of "T-1", A242, and A 7 columns

6. Especially in the case of the solid round bars but also in the welded A7 box shapes, it has been necessary to take into account initial out-of-straightness to satisfactorily explain the observed load-carrying capacity, Figures 26 and 27. For the "T-1" steel members, the influence of residual stress is less pronounced, whereas that of initial crookedness is increased. In part, these variations offset one another, and in part, it might be the basis for using a somewhat higher design stress for medium length columns.

On the basis of this research, we can now accurately predict the strength of steel columns. Figure 30 shows all of the available test data on a nondimensional basis to eliminate yield stress as a variable. The CRC's basic column curve is also shown. In Figure 31 the same data are plotted, making use of available theory to take into account (1) residual stresses due to cooling after rolling, welding, and heat treating, (2) cold-bending residual stresses, (3) strain-hardening, (4) initial out-of-straightness, and (5) different yield stresses. The agreement between the experimental values and the predicted values is very good.

ACKNOWLEDGMENT. The research at Lehigh University on round bars is currently being sponsored by the United States Steel Corporation. The work on rolled and welded shapes is being done under sponsorship of the Column Research Council with a major portion of the financing by the Pennsylvania Department of Highways and the United States Department of Commerce, Bureau of Public Roads.

References

1. L. S. Beedle and L. Tall, "Basic Column Strength," Proceedings ASCE, 86, ST7, July 1960.
2. L. Tall, "The Strength of Welded Built-Up Columns," Ph.D. Dissertation, Lehigh University, 1961.
3. A. Nitta, "Ultimate Strength of High Strength Steel Circular Columns," Ph.D. Dissertation, Lehigh University, 1960.
4. Memorandum, "The Basic Column Formula," Column Research Council, Tech. Memorandum No. 1, May 1952.